Research on Chemical Intermediates
https://doi.org/10.1007/s11164-020-04240-6

Synthesis of quinoxaline, benzimidazole and pyrazole derivatives under the catalytic influence of biosurfactant-stabilized iron nanoparticles in water

Satyanarayan M. Arde[1] · Audumbar D. Patil[1,2] · Ananda H. Mane[3] · Prabha R. Salokhe[4] · Rajashri S. Salunkhe[1]

Received: 17 February 2020 / Accepted: 12 August 2020

Abstract

We have reported the synthesis, characterization, and catalytic applications of amorphous iron nanoparticles (FeNPs) using aqueous leaves extract of renewable natural resource *Boswellia serrata* plant. Synthesized FeNPs were stabilized in situ by the addition of aqueous pod extracts of *Acacia concinna* as a biosurfactant (pH 3.11). The structural investigation of biosynthesized nanoparticles was performed using UV–visible spectroscopy, X-ray diffraction analysis, selected area electron diffraction, energy-dispersive X-ray spectroscopy, scanning electron microscopy, transmission electron microscopy, X-ray photoelectron spectroscopy, thermogravimetric analysis, and BET analysis. The FeNPs were amorphous in nature with average particle size ~ 19 nm and successfully employed as heterogeneous catalyst for the synthesis of quinoxaline, benzimidazole, and pyrazole derivatives in aqueous medium at ambient conditions. The FeNPs could be recycled up to five times with modest change in the catalytic activity.

Electronic supplementary material The online version of this article (https://doi.org/10.1007/s11164-020-04240-6) contains supplementary material, which is available to authorized users.

✉ Rajashri S. Salunkhe
rsschem1@gmail.com

[1] Department of Chemistry, Shivaji University, Kolhapur, MS 416004, India

[2] Department of Chemistry, School of Science, Sanjay Ghodawat University, Kolhapur, MS, India

[3] Department of Chemistry, KIT's College of Engineering, Kolhapur, MS 416234, India

[4] Department of Chemistry, Y. C. Warana Mahavidyalaya, Warananagar, MS 416113, India

Published online: 28 August 2020

Graphic abstract

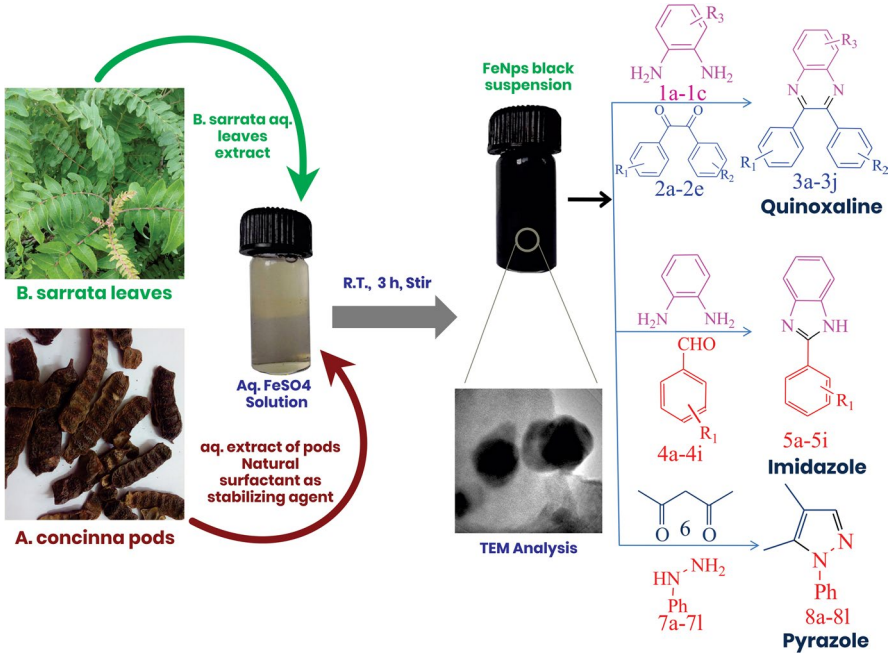

Keywords Amorphous iron nanoparticles · Bioreduction · *Boswellia serrata* · Stability of FeNPs · Biosurfactant · *N*-heterocyclic compounds · Aqueous medium

Introduction

The green synthesis of metallic nanoparticles (NPs) has garnered tremendous attention in the scientific community, due to the growing environmental contamination caused by the conventional chemical methods [1]. Usually, NPs have been synthesized using various chemical and physical methods based on the availability and feasibility of protocols to achieve the required applications [2–5]. However, some of these methods include use of expensive equipment and hazardous chemicals which have harmful effects with respect to environment and human health. Moreover, during the chemical synthesis, the residuals of some toxic chemicals may adsorb on the surfaces of the NPs, which prevent their application in biomedical equipment [6]. Therefore, there is immense interest in the development of environmentally friendly and sustainable methods for the preparation of NPs.

From the literature survey, plenty of reports are available on the synthesis of metal NPs using bacteria, fungi, microorganisms, and plant extract [7–11]. Amid various biogenic syntheses of NPs, use of plant extract could be more advantageous as it does not involve elaborative process and repeated growth of cell culture of microbes and their

maintenance [12]. It was already explored that the rate of metal ion reduction by plant extract is much faster than the microorganism [13]. The biomolecules in plant extract like proteins, phenols, flavonoids, etc. play the crucial role for the reduction of metal ions [14], but sometimes plant extracts do not produce stable NPs like magnetic NPs because they have high propensity to aggregate leading to get larger particle size due to small surface area. To avoid the agglomeration of magnetic NPs, synthetic stabilizing agents (surfactants) could be used [15], but the green chemistry principles do not allow the synthetic surfactants as they might not be ecofriendly. To overcome this difficulty, biosurfactants like aqueous extract of *Acacia concinna* pods play crucial role in the stabilization of magnetic nanoparticles.

Functionalized magnetic NPs have great interest due to their unique properties and its wide spread applications [16, 17]. It is a renowned material in the field of catalysis over the last decade as they have combine interesting reactivity with an easy, economical and environmentally benign mode of recovery [18]. In particular, zero-valent FeNPs represent a wide range of peculiar applications in different fields such as magnetic resonance imaging [19], Raman scattering and electrocatalysis [20], remediation of aqueous metal contaminants [21], potential magnetic carriers [22], declorination [23], imine synthesis [24], chromium removal [25], etc.

Considering aforementioned discussion and importance of FeNPs, in present work, we describe a facile and environmentally friendly technique for the preparation of FeNPs using an aqueous extract of *Boswellia sarrata* L. leaves as a bioreductant and Acacia concinna pods as stabilizing agent. Furthermore, biosynthesized FeNPs were successfully employed as a heterogeneous catalyst in one-pot multicomponent synthesis of quinoxaline benzimidazole and pyrazole derivatives. Quinoxaline, benzimidazole, and pyrazole scaffolds containing molecules have considerable biological and pharmacological properties [26, 27]. The heterocyclic imidazole nucleus is the most important scaffolds due to their medicinal properties [28] and found in a number of naturally occurring compounds such as histamine, histidine, pilocarpine, allantoin, and vitamin B_{12} [29]. In addition, pyrazole moiety is used as a precursor for the synthesis of compounds presenting many applications such as electrolyte additives in batteries, catalysis, photographic materials, agrochemicals, dyes and as a versatile compound used in medicine [30]. Nevertheless, in the traditional approaches of quinoxaline synthesis using di-carbonyls with the diamine molecules, use of expensive reactive reagents, poor yields, harsh reaction conditions are the major issues that have been reported. In continuation of our previous research work [31–35], development of sustainable methodology for heterocycle synthesis, herein we have reported synthesis of quinoxaline, benzimidazole, and pyrazole derivatives by using biosurfactant-stabilized FeNPs. Addition of *Acacia concinna* aqueous pod extract (a stabilizing agent), affected the stability of FeNPs, and it remained in suspended form for weeks in aqueous solution.

Experimental

General information

All reagents were purchased from Sigma-Aldrich and used without further purification. All reagents were weighed and handled in the air at room temperature. Fresh, green, and mature leaves of *Boswellia serrata* and pods of *Acacia concinna* were collected from "Western Hilly Region" of Maharashtra (India), and the taxonomic identification was made in Department of Botany, Shivaji University, Kolhapur (MS, India). The voucher specimen was numbered (SMA 001) and kept in our research laboratory for further reference. The aqueous extract of *Boswellia sarrata* leaves and *Acacia concinna* pods were freshly prepared using double distilled water and kept in dark at room temperature for further use. The UV–visible spectra were recorded over 200–800 nm range with UV-3600 PC UV–VIS NIR Spectrophotometer (Shimadzu). XRD patterns were recorded on Bruker AXS model D-8, (10°–70° range, scan rate = 1° min^{-1}) equipped with a monochromator and Ni-filtered Cu Kα radiation. SEM was performed using a HITACHI S-4800 instrument to study the morphology of FeNPs. The TEM analysis was performed on a Jeol model JEM 1200 electron microscope operated at an accelerating voltage of 120 kV. The EDS was carried out on a DX-700HS spectrometer for elemental analysis. XPS data of catalyst were collected on a VG scientific ESCA-3000 spectrometer using a non-monochromatized Mg K radiation (1253.6 eV) at a pressure of about 1×10^{-9} Torr (Pass energy of 50 eV, electron takeoff angle 55°). BET surface area of adsorbants was determined by N2 adsorption–desorption techniques using Micromeritics-2720 (Chemisoft TPx) volumetric instruments. Melting points were determined in an open capillary and were uncorrected. ^{1}H NMR spectra were recorded at 300 MHz Bruker Avon spectrometer using $CDCl_3$ as solvent and TMS as an internal reference. IR spectra were recorded on Thermo Scientific Neconet 6700 FTIR, in the range 4000–400 cm^{-1}. Mass spectra were performed on an Ultima Global spectrometer with an ESI source.

General procedure for the synthesis of FeNPs

Diluted aqueous extract of *Boswellia sarrata* leaves (25 mL) was added drop wise to 25 mL of ferrous sulfate solution (1 mM) containing 10 mL of *Acacia concinna* pod aqueous extract at room temperature with constant stirring for 3 h. *Acacia concinna* pod aqueous extract, a natural surfactant, acted as a stabilizing as well as capping agent and prevented the agglomeration of FeNPs. The color of $FeSO_4$ aqueous solution gradually changed from light yellow to black indicated the formation of FeNPs upon addition of an aqueous solution of plant extract (PE) (Fig. 1). The obtained black solution was centrifuged at 10,000 rpm for 20 min and then washed with distilled water (3 × 10 mL). The black solid obtained was dried under vacuum and used for further study.

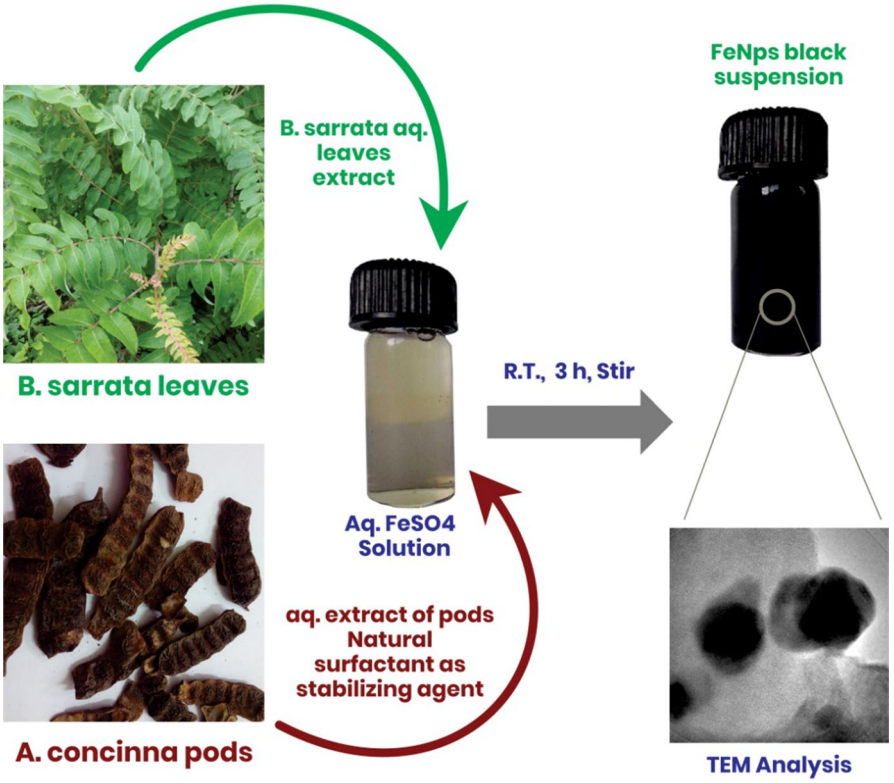

Fig. 1 Preparation of FeNPs by the exposure of $FeSO_4$ aqueous solution with *B. serrata* aqueous leaves extract and *A. concinna* aqueous pod extract as stabilizing agent

General procedure for the synthesis of quinoxaline/imidazole

A 25 mL round-bottom flask was charged with a mixture of Benzil/aldehyde (1 mmol), ortho phenylene diamine (OPD) (1 mmol) and 5 mol% of FeNPs. The mixture was stirred in water at room temperature (31 °C) about 5–10 min. The completion of reaction was monitored by TLC and solid was separated by filtration/centrifuge, on pouring the mixture into ice cold water. The obtained product was recrystallized in ethanol to afford the pure product.

General procedure for the synthesis of pyrazole

A 25 mL round-bottom flask was charged with a mixture of acetyl acetone (1 mmol), phenyl hydrazine (1 mmol) and 5 mol% of FeNPs. The mixture was stirred in water at room temperature (31 °C) about 5–10 min. The completion of reaction was monitored on TLC and solid was separated by filtration/centrifuge,

on pouring the mixture into ice cold water. Obtained product was recrystalized in ethanol to afford the pure product.

Results and discussion

Initially, the black suspension of biosynthesized material was monitored via UV–Vis spectroscopy. Figure 2 displayed the UV–visible spectra of (a) *Boswellia serrata* aqueous PE, (b) *Acacia concinna* aqueous pod extract, (c) $FeSO_4$ aqueous solution and (d) FeNPs black suspension at room temperature after 3 h. The strong surface plasmon resonance band of $FeSO_4$ appeared at 345 nm (c) was disappeared in (d) spectra indicated that complete reduction of Fe^{++} to Fe^0 within 3 h converting gradually faint yellow solution into black suspension.

Next, we have studied the physical parameters with respect to pH and potential difference of the PE, surfactant, and black suspension before and after completion of the reaction and results are summarized in Table 1a, b.

According to electrochemical series, it is indicated that Fe^{++} ions can be reduced when PE or any other reducing agents should have potential difference (reduction potential) greater than −0.41. Considering above statement, fortunately, potential difference of aqueous extract of *Boswellia sarrata* leaves was found to be −0.65 V, and hence reduction of Fe^{++} could be possible by the selected plant material.

As synthesized nanoparticles were agglomerated in the solution, stability of material checked in different biosurfactants and results are displayed in Table 2. From Table 2, it is concluded that, *Acacia concinna* aqueous pod extract (acidic biosurfactant, pH 3.11) is suitable stabilizing agent for the synthesis of FeNPs that is stability of respective nanoparticles is pH sensitive. Thus it can be presumed that plant extract with high reductant capacity and acidic pH will be best suited for the synthesis of iron nanoparticles [15].

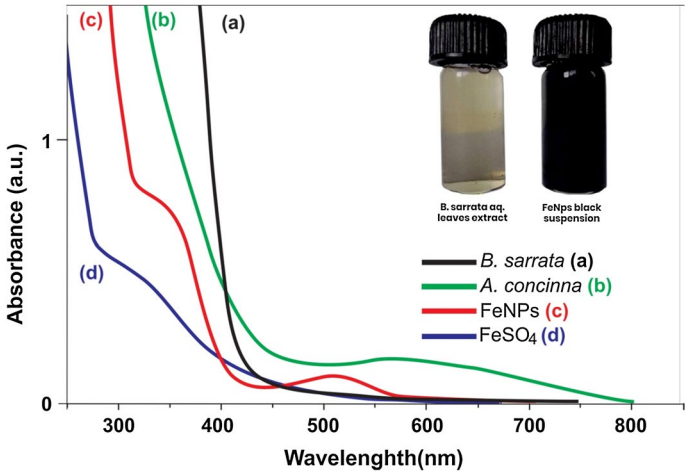

Fig. 2 UV–visible spectra of biosynthesized nanomaterials

Table 1 Study of (a) pH change, (b) potential difference change

S. no.	Solutions	pH
(a)		
1.	*Boswellia sarrata* leaves aq. extract	4.36
2.	*Acacia concinna* pod aq. extract	3.11
3.	$FeSO_4$ Solution	5.01
4.	Black suspension of synthesized nanomaterials	3.05
S. no.	Solutions	Potential difference
(b)		
1.	*Boswellia sarrata* leaves aq. extract	−0.650
2.	*Acacia concinna* pod aq. extract	+0.085
3.	$FeSO_4$ solution	+0.040
4.	Black suspension of synthesized nanomaterials	+0.175

Table 2 The effect of biosurfactants toward the stability of the iron nanoparticles

S. no.	Biosurfactant	pH	Stability toward biosynthesized FeNPs
1.	*Sapindus mukorossi* (Ritha)	6.43	Not stable
2.	*Balanites rosburghii*	5.54	Not stable
3.	*Acacia concinna*	3.11	Stable

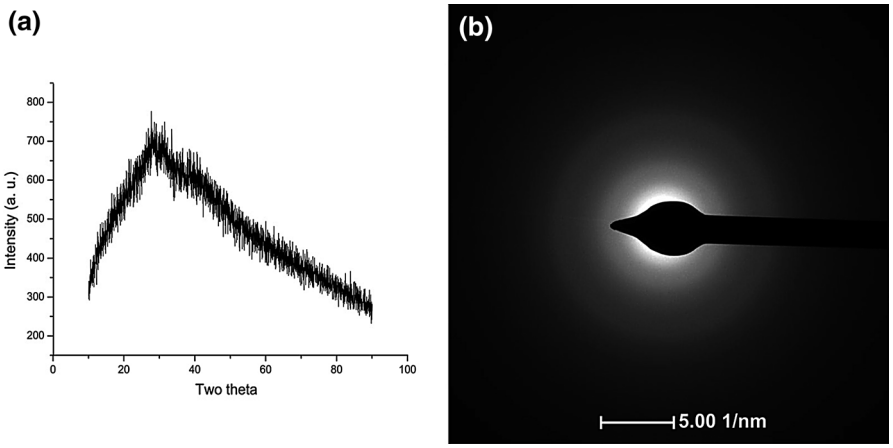

Fig. 3 **a** XRD pattern and **b** SAED Pattern of biosynthesized nanomaterials

The XRD report of biosynthesized FeNPs (Fig. 3a) showed the dense descending slope with no sharp peaks. Lack of distinct XRD pattern suggesting that FeNPs are amorphous in nature and for ultra-small crystalline materials where diffraction peaks cannot be well resolved. In support to this, the SAED pattern/micrograph does

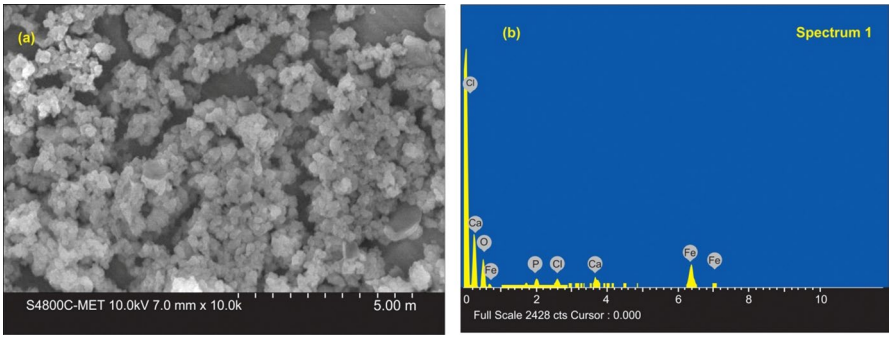

Fig. 4 **a** SEM and **b** EDS spectrum of biosynthesized nanomaterials

not have any clear diffraction rings or spot pattern but show a diffuse ring confirming the FeNPs is amorphous in nature (Fig. 3b).

The morphology of biosynthesized nanomaterials has been confirmed from SEM study. The FE-SEM image (Fig. 4a) indicated the formation of the rectangle and nearly uniform sized FeNPs. Elemental analysis was carried out by using EDS analysis (Fig. 4b). The presence of a great deal of Fe atoms with other atoms including phosphorous, calcium, oxygen, chlorine [36] is clearly evident from the spectrum, which indicates the presence of residual phytomolecules of the plant extract as capping ligands on the surfaces of the FeNPs. Biosynthesized black powder on EDS analysis displays an optical absorption peak at 6.4 keV, which is typical of the absorption of iron.

The uniformity and particle size of biosynthesized FeNPs were investigated using TEM analysis (Fig. 5) and particle size distribution graph. The particles are distributed in the range 15–25 nm. According to the electron micrographs, the FeNPs is predominantly rectangular/oval in shape with an average particle size of 19 ± 3 nm.

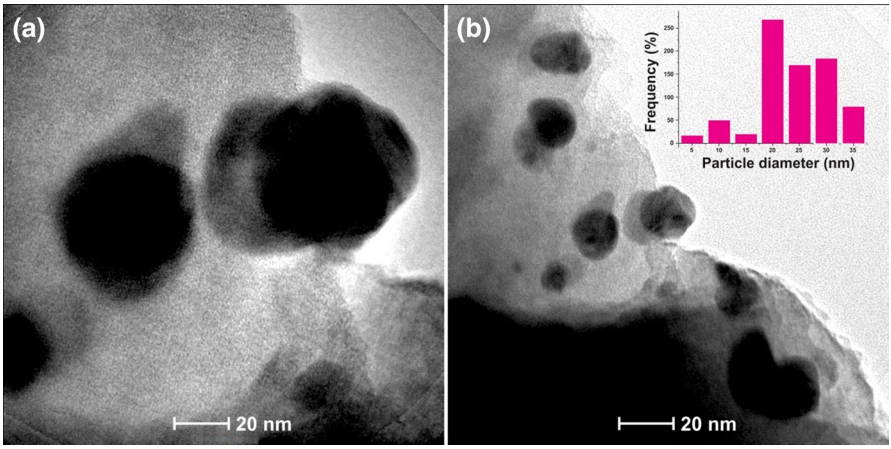

Fig. 5 TEM image of FeNPs with particle size distribution graphs

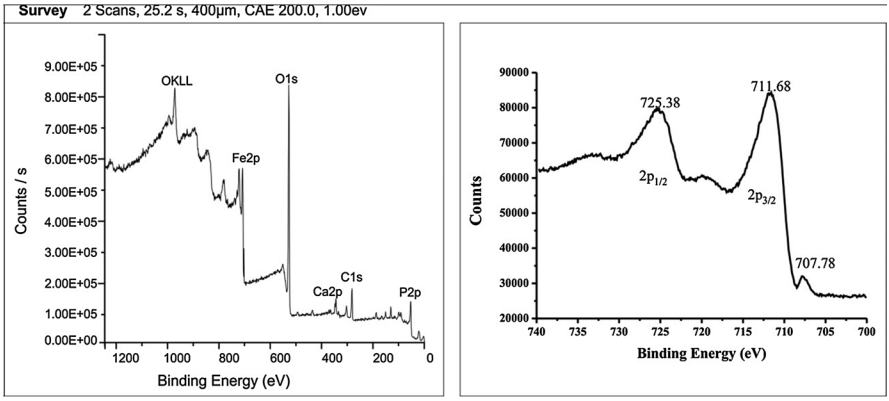

(a) Full survey XPS **(b)** XPS spectrum of Fe 2p-electrons

Fig. 6 **a** Full survey XPS and **b** XPS spectrum of Fe 2*p*-electrons

Fig. 7 TGA analysis of FeNPs

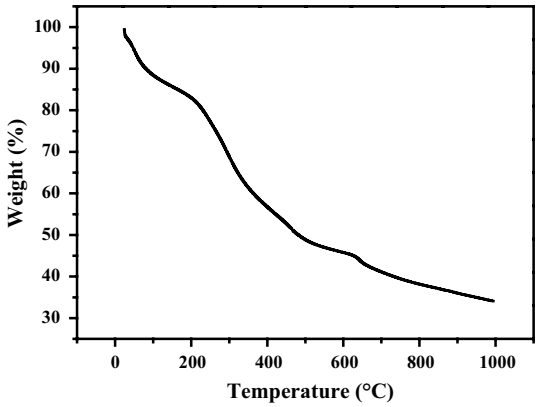

The presence some larger particles can be attributed to the aggregation or overlapping of smaller particles.

BET analysis provides precise specific surface area evaluation of the materials. The biosynthesized FeNPs found that BET surface area equals to 59 m^2/g.

Overview of XPS spectrum of iron containing NPs produced from *Boswellia serrata* aqueous leaves extract (Fig. 6), indicates lines of carbon, oxygen, phosphorus, iron, and nitrogen. In the XPS spectrum of Fe 2*p*-electrons (Fig. 6b), distinct states of the iron atoms at 711.68 eV was observed, which correspond to the binding energy electron components of Fe 2*p*3/2. Such binding energies were typical for trivalent and divalent iron atoms respectively[25]. However, the absence of a distinct satellite peak could be observed in Fig. 6b. There was a mild peak at 707.78 eV, corresponding to Fe^0. As the Fe nanoparticles were exposed to the air in the process of sample preparation and testing, the Fe^0 was oxidized, hence the weakness of the peak at 707.78 eV. Therefore, the nanoparticles synthesized in

extracts of *Boswellia serrata* aqueous leaves extract mainly contained nano-Fe_3O_4 and Fe^0 based on XPS spectrum.

In the TGA curve (Fig. 7), it was observed that three regions with different slopes are recognized. In the first region 40–153°C, weight loss is attributed to the vaporization of water and the degradation of volatile organic materials loosely bonded on the surface of the FeNPs. Further increase in heat flow results in progressive weight loss which indicates that the FeNPs material is unstable at high temperature.

With the above characterization, catalytic activity of FeNPs has explored for the synthesis of biological active *N*-heterocyclic compounds namely quinoxalines, benzimidazole and pyrazole derivatives in water at room temperature. As aqueous media propose many practical, economical, and ecological advantages over organic solvents, it is beneficial to use as a reaction solvent because it is safe, harmless, and environmentally friendly [37].

Catalytic activity of FeNPs firstly tested with the synthesis of quinoxaline. The condensation reaction of benzil with ortho phenylene diamine (OPD) was used as a model reaction to investigate the catalytic performance of FeNPs and the effect of media upon the reaction. In the absence of catalyst the product 3a (Table 5, entry 1) was produced with very trace amount after 10 h of stirring in water (Table 3, entry 1), but on addition of FeNPs (5 mol% in comparison with

Table 3 Optimization studies for the synthesis of quinoxaline

S. no.	Reaction medium	FeNPs (mol%)	Time	Reaction condition	Yield[a] (%)
1	Water	–	10 h	r.t./reflux	Trace
2	Ethanol	–	10 h	r.t./reflux	Trace
3	Acetonitrile	–	10 h	r.t./reflux	Trace
4	DMF	–	10 h	r.t./reflux	Trace
5	Acetone	–	10 h	r.t./reflux	Trace
6	H_2O	5	5 min	r.t.	98
7	Ethanol:water (1:1)	5	8 min	r.t.	95
8	Ethanol	5	15 min	r.t.	81
9	Acetone	5	20 min	r.t.	80
10	Acetone:water (1:1)	5	15 min	r.t.	90
11	DMF	5	20 min	r.t.	68
12	CH_3CN	5	30 min	r.t.	60

Reaction conditions: benzil (1 mmol), *o*-phenylenediamine (1 mmol), Solvent (5 mL), FeNPs (catalytic amount)

[a]Isolated yield

the other reported catalyst [38, 39]) in reaction mixture, conversion of substrate to product was suddenly increased up 98% in 5 min (Table 3, entry 6). There is a noticeable difference in the product yield between water and organic solvent. This might be due to dispersion of catalyst in the solvent. Biosynthesized FeNPs was amorphous in nature (Fig. 3) and well dispersed in the water, whereas in organic solvent, it was aggregated and settled down. This might be the reason that the yield of the product is low in organic solvent as compared to water.

With these results in hand, we have determined the FeNPs concentration for maximum yield of the product in water. Thus, the model reaction was carried out with various concentrations (mol%) of FeNPs in water at ambient temperature. By changing concentration, dramatic effect on the conversion rate of quinoxaline has been observed. As shown in Table 4, linear relationship was observed with concentration. The yield of the product is highest at 5 mol% of FeNPs catalyst. On the other hand, further increase in concentration resulted in no increase or decrease in the product yield.

To explore the scope and generality of the catalyst, the optimized protocol [*o*-phenylenediamine (1.0 mmol), benzil (1.0 mmol), water (5 mL), at room temperature under air] was applied for reactions of variety of *o*-phenylenediamine and 1,2 diketone with moderate to excellent yield (80–98%).

According to experimental results, high reaction rates and yields were obtained with both activated and non-activated benzils (Table 5, entry 1–10). Benzils without any substituent and activated benzils with electron-withdrawing substituents are reactive substrates in quinoxaline synthesis and the related reactions went to completion in shorter reaction times. As an example, the reaction of benzil with OPD completed within 5 min giving the desired product in 98% isolated yield (Table 5, entry 1). Non-activated benzil with electron-donating substituent on the aromatic ring are not reactive substrates in quinoxaline synthesis and related reactions completed in longer reaction times (Table 5 in entry 3).

Inspired from these results, we have explored the scope of FeNPs for the synthesis of benzimidazole, instead of benzil, benzaldehyde was reacted with OPD (Scheme 1) at room temperature in aqueous medium. Reaction was completed within 5 min with excellent yield in aqueous medium with use of 5 mol% of catalyst. To explore the scope and generality of the catalyst, the optimized protocol for

Table 4 Optimization of catalyst for quinoxaline synthesis

Entry	Catalyst (mol%)	Time (min)	Yield[a] (%)
1	1	45	40
2	2	25	52
3	3	15	75
4	4	15	84
5	5	5	98
6	6	5	98

Reaction conditions: *o*-phenylenediamine (1 mmol), benzil (1 mmol), water (5 mL), RT

[a]Isolated yields after purification

Table 5 Synthesis of quinoxaline and its derivatives by FeNPs

Entry	1,2-diamine	1,2-diketone	Product	Time (min)	Yield[a] (%)
1	 1a	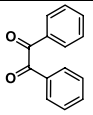 2a	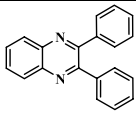 **3a**	5	98
2	 1a	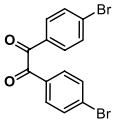 2b	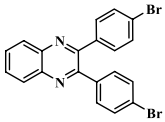 **3b**	12	91
3	 1a	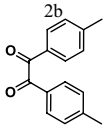 2c	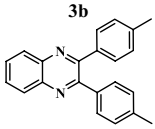 **3c**	15	85
4	 1a	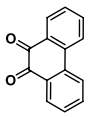 2d	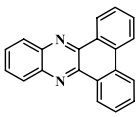 **3d**	7	93
5	 1a	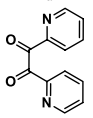 2e	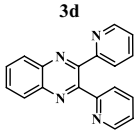 **3e**	15	92
6	 1b	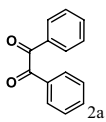 2a	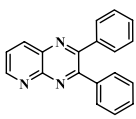 **3f**	25	80
7	 1b	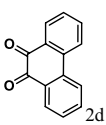 2d	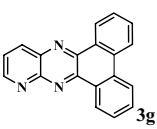 **3g**	25	86
8	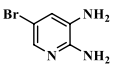 1c	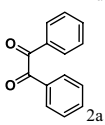 2a	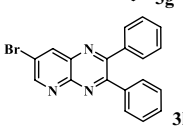 **3h**	10	92
9	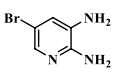 1c	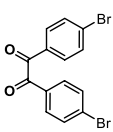 2b	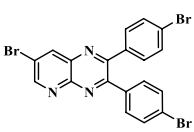 **3i**	25	92
10	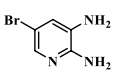 1c	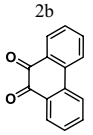 2d	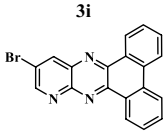 **3j**	10	93

Table 5 (continued)

Reaction conditions: diketone (1 mmol), OPD (1 mmol), FeNPs catalyst (5 mol%), water 5 mL, RT

[a]Isolated yields

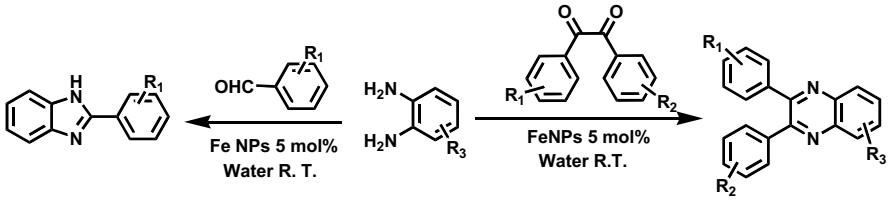

Scheme 1 Synthesis of quinoxaline and benzimidazole

benzimidazole was applied for reactions of variety of aldehydes and *o*-phenylenediamine with moderate to excellent yield (93–78%) (Table 6).

Pyrazole is one of the five member heterocyclic compound containing two nitrogen atoms present at 1, 2 positions. We also tried for the synthesis of pyrazole in the presence of FeNPs as a catalyst in aqueous medium at room temperature. The results obtained are summarized in Table 7. The optimized protocol was applied for reactions of variety of phenyl hydrazine and acetyl acetone with moderate to excellent yield (92–75%).

Plausible reaction mechanism

The plausible reaction mechanism for the synthesis of quinoxaline derivatives are shown in Scheme 2. The mechanism proceeds by oxidative addition of FeNPs on carbonyl oxygen of benzil (**1**) followed by the nucleophilic attack of lone pair of nitrogen of OPD (**2**, **3**) on activated carbonyl carbon. Same process of mechanism (**4**) is repeated for second carbonyl oxygen of benzil to form six membered cyclic intermediate (**5**). Further, the six-membered cyclic intermediate (**5**) abstract protons from solvent leaving behind FeNPs to form dihydroxy intermediate (**6**). This (**6**) on dehydration yields desired product (**7**).

Table 6 Synthesis of benzimidazoles its derivatives in aqueous medium by using 5 mol% FeNPs

Entry	Aldehyde	Product	Time (Min)	Yield[a] (%)
1	 4a	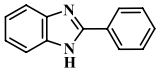 **5a**	5	93
2	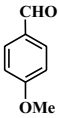 4b	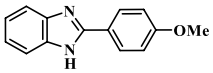 **5b**	30	83
3	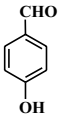 4c	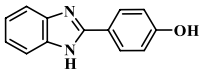 **5c**	25	78
4	 4d	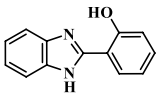 **5d**	25	80
5	 4e	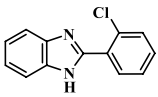 **5e**	25	86
6	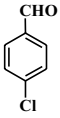 4f	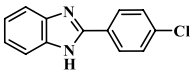 **5f**	30	88
7	 4g	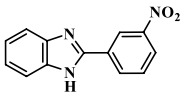 **5g**	15	87
8	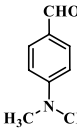 4h	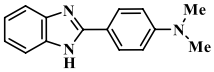 **5h**	20	88
9	 4i	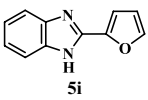 **5i**	20	80

Reaction conditions: aldehyde (1 mmol), *o*-phenylenediamine (1 mmol), FeNPs catalyst (5 mol%), water 5 mL, RT

[a]Isolated yields after recrystallization

Table 7 Synthesis of pyrazoles in aqueous medium by using 5 mol% FeNPs

Entry	Hydrazine/ Hydrazide	Product	Reaction Time (min)	Yield[a] (%)
1	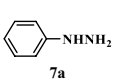 **7a**	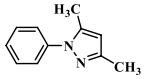 **8a**	15	92
2	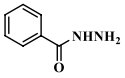 **7b**	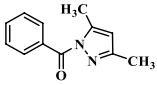 **8b**	30	87
3	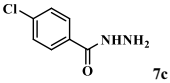 **7c**	 **8c**	40	82
4	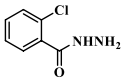 **7d**	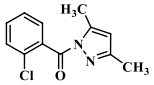 **8d**	80	80
5	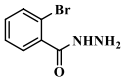 **7e**	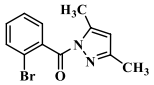 **8e**	90	78
6	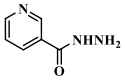 **7f**	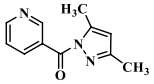 **8f**	30	77
7	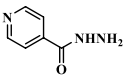 **7g**	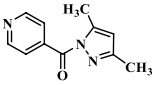 **8g**	50	83
8	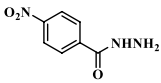 **7h**	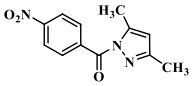 **8h**	5 h	77
9	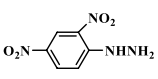 **7i**	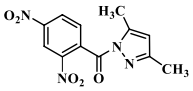 **8i**	12 h	75
10	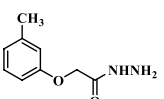 **7j**	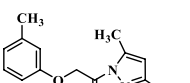 **8j**	40	84
11	$NH_2NH_2.H_2O$ **7k**	 **8k**	15	90
12	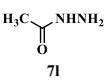 **7l**	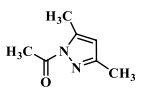 **8l**	25	90

Table 7 (continued)

Reaction conditions: phenyl hydrazine (1.2 mmol), reaction medium (5 mL), acetyl acetone (1 mmol), FeNPs (5 mol%)

[a]Isolated yields

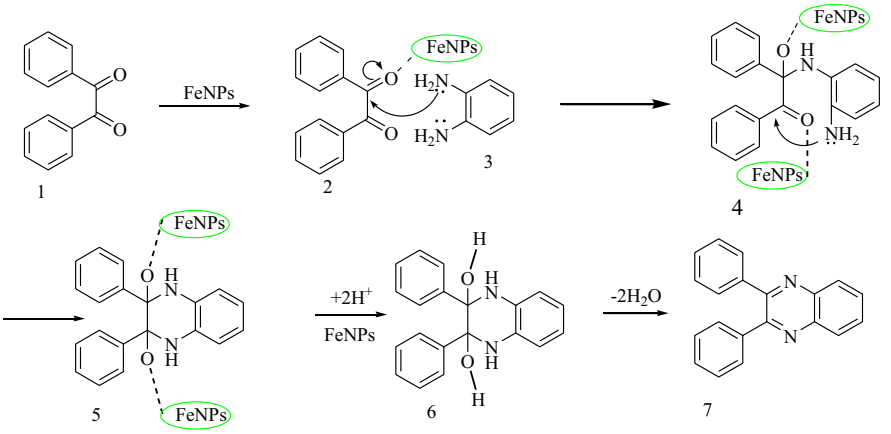

Scheme 2 Plausible reaction mechanism for quinoxaline model reaction (Table 5, entry 1)

Reusability

For practical applications of homogeneous systems, the lifetime of the catalyst and its level of reusability are very important features. The recyclability of catalyst was investigated with consecutive quinoxaline synthesis by taking *o*-phenylenediamine (1 mmol), benzil (1 mmol) in aqueous medium at room temperature. After the completion of first cycle, the product was extracted by ethyl acetate and the catalyst was recovered by centrifugation and extensively washed

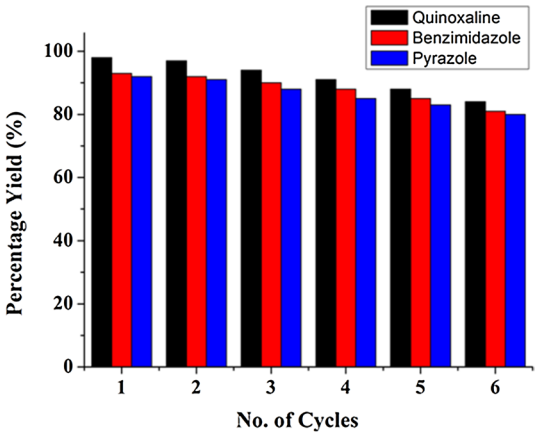

Fig. 8 Reusability of FeNPs catalyst in quinoxaline, pyrazole, and imidazole synthesis

with water, dichloromethane and acetone. The catalyst was then dried under vacuum before performing the reusability test. The recycling results of catalyst were summarized in Fig. 8. After the first cycle, activity of catalyst is decreased with decreasing yield from 98 to 84% with increased time. The same process was repeated in the syntheses of benzimidazole and pyrazole and the collective reusability graph is shown below.

Conclusions

In summary, we have demonstrated an efficient, simple, economical and environmentally benign protocol for the synthesis of FeNPs by using *Boswellia serrata* aqueous leaves extract and its catalytic applications in the synthesis of quinoxalines, benzimidazole and pyrazole derivatives in an aqueous medium at room temperature. Biosynthesized FeNPs were stabilized in aqueous pod extract of *Acacia concinna*, a natural surfactant (pH 3.11). The size of FeNPs was characterized by TEM analysis and it was ~ 19 nm. The amorphous nature of FeNPs was analyzed by XRD and SAED analysis and used as a non-toxic, inexpensive, heterogeneous catalyst in an aqueous medium. It was recycled up to five cycles with modest change in catalytic activity. Thus, the catalytic protocol developed provides an unprecedented reactivity pattern, an economically attractive and environmentally benign alternative route for the production of quinoxaline, benzimidazole, pyrazole and widens the synthesis of related compounds in organic syntheses.

References

1. M. Khan, M. Khan, M. Kuniyil, S.F. Adil, A. Al-Warthan, H.Z. Alkhathlan, W. Tremel, M.N. Tahir, M. Rafiq, H. Siddiqui, Dalton Trans. **43**, 9026 (2014)
2. O.A. Guselnikova, A.I. Galanov, A.K. Gutakovskii, P.S. Postnikov, Beilstein J. Nanotechnol. **6**, 1192 (2015)
3. J. Ruusunen, M. Ihalainen, T. Koponen, T. Torvela, M. Tenho, J. Salonen, O. Sippula, J. Joutsensaari, J. Jokiniemi, A. Lahde, J. Nanopart. Res. **16**, 2270 (2014)
4. M. Kim, K. Park, T. Lim, S. Choe, T. Yu, J.J. Kim, J. Electrochem. Soc. **160**(1), E1 (2013)
5. A. Szpak, G. Kania, T. Skorka, W. Tokarz, S. Zapotoczny, M. Nowakowska, J. Nanopart. Res. **15**, 1372 (2013)
6. K. Byrappa, S. Ohara, T. Adschiri, Adv. Drug Deliv. Rev. **60**, 299 (2008)
7. R. Oremland, M. Herbel, J. Blum, S. Langley, T. Beveridge, P. Ajayan, T. Sutto, A. Ellis, S. Curran, Appl. Environ. Microbiol. **70**(1), 52 (2004)
8. K. Narayanan, N. Sakthivel, Adv. Colloid Interface Sci. **156**, 1 (2010)
9. K.V. Pavani, N.S. Kumar, Am. J. Nanomater. **1**(2), 24 (2013)
10. S.M. Arde, P.R. Salokhe, A.H. Mane, R.S. Salunkhe, Chem. Sci. Rev. Lett. **3**(11), 557 (2014)
11. N.L. Gavade, A.N. Kadam, M.B. Suwarnkar, V.P. Ghodake, K.M. Garadkar, Spectrochim. A Mol. Biomol. Spectrosc. **136**, 953 (2015)
12. T. Santhoshkumar, A.A. Rahuman, A. Bagavan, S. Marimuthu, C. Jayaseelan, A.V. Kirthi, C. Kamaraj, G. Rajakumar, A.A. Zahir, G. Elango, K. Velayutham, M. Iyappan, C. Siva, L. Karthik, K.V.B. Rao, Exp. Parasitol. **132**, 156 (2012)
13. S. Iravani, Green Chem. **13**, 2638 (2011)

14. S. Gnanasekar, G. Chandrakasan, K. Karuppiah, H. Vedagiri, P. Kumpati, S. Sivaperumal, Colloids Surf. B Biointerfaces **95**, 235 (2012)
15. V.V. Makarov, S.S. Makarova, A.J. Love, O.V. Sinitsyna, A.O. Dudnik, I.V. Yaminsky, M.E. Taliansky, N.O. Kalinina, Langmuir **30**(20), 5982 (2014)
16. S. Peng, C. Wang, J. Xie, S. Sun, J. Am. Chem. Soc. **128**, 10676 (2006)
17. E. Carenza, V. Barcelo, A. Morancho, J. Montaner, A. Rosell, A. Roig, Acta Biomater. **10**, 3775 (2014)
18. Y. Sun, X. Li, J. Cao, W. Zhang, H.P. Wang, Adv. Colloid Interface Sci. **20**, 47 (2006)
19. S. Cheong, P. Ferguson, K. Feindel, I. Hermans, P. Callaghan, C. Meyer, A. Slocombe, C. Su, F. Cheng, C. Yeh, B. Ingham, M. Toney, R. Tilley, Angew. Chem. Int. Ed. **50**, 4206 (2011)
20. L. Guo, Q. Huang, X. Li, S. Yang, Phys. Chem. Chem. Phys. **3**, 1661 (2001)
21. S. Ponder, J. Darab, J. Bucher, D. Caulder, I. Craig, L. Davis, N. Edelstein, W. Lukens, H. Nitsche, L. Rao, D. Shuh, T. Mallouk, Chem. Mater. **13**, 479 (2001)
22. E.E. Carpenter, J. Magn, Magn. Mater. **225**, 17 (2001)
23. C. Wang, W. Zhang, Environ. Sci. Technol. **31**(7), 2154 (1997)
24. G. Jaiswal, V.G. Landge, D. Jagadeesan, E. Balaraman, Green Chem. **18**, 3232 (2016)
25. Y. Wei, Z. Fang, L. Zheng, E.P. Tsang, Appl. Surf. Sci. **399**, 322 (2017)
26. C. Antonio, P. Giuseppe, M. Nikookar, S. Paolo, S. Leonardo, Z. Stefania, Eur. J. Med. Chem. **37**, 355 (2002)
27. B. Gao, D. Xia, Y. Geng, Y. Cheng, L. Wang, Tetrahedron Lett. **51**, 1919 (2010)
28. S. Bhattacharya, P. Choudhuri, Curr. Med. Chem. **15**, 1762 (2008)
29. S.B. Kamble, G.S. Rashinkar, A.S. Kumbhar, K.B. Mote, R.S. Salunkhe, Synth. Commun. **42**(5), 756 (2012)
30. D. Kam, K. Kim, H. Liu, Electrochem. Commun. **11**, 1657 (2009)
31. A. Patil, R. Salunkhe, Res. Chem. Intermed. **44**, 3337 (2018)
32. T. Lohar, A. Kumbhar, A. Patil, S. Kamat, R. Salunkhe, Res. Chem. Intermed. **45**, 639 (2019)
33. A. Patil, A. Mane, S. Kamat, T. Lohar, R. Salunkhe, Res. Chem. Intermed. **45**, 3441 (2019)
34. A. Patil, S. Gajare, G. Rashinkar, R. Salunkhe, Catal. Lett. **150**, 127 (2020)
35. A. Patil, T. Lohar, A. Mane, S. Kamat, R. Salunkhe, J. Heterocycl. Chem. **56**, 3145 (2019)
36. R. Bawankar, P. Singh, B. Subramanian, J. Plant Sci. **2**, 102 (2014)
37. S. Venkateswarlu, B.N. Kumar, C.H. Prasad, P. Venkateswarlu, N.V.V. Jyothi, Phys. B **449**, 67 (2014)
38. K. Holmberg, Curr. Opin. Colloid Interface Sci. **8**, 187 (2003)
39. A.R. Siamaki, B.A. Arndtsen, J. Am. Chem. Soc. **128**, 6050 (2006)